JJEE
Volume 11 | Number 4 | Pages 806-823

Jordan Journal of Electrical Engineering

ISSN (print): 2409-9600, ISSN (online): 2409-9619

Homepage: jjee.ttu.edu.jo

Optimizing Voltage Profiles through Smart Inverter Volt/VAR Control in PV-Enriched Distribution Networks

Dhaval Yogeshbhai Raval[1*], Saurabh N. Pandya[2]

[1] Ph.D. Scholar, Gujarat Technological University, Chandkheda, Ahmedabad, Gujarat, India
E-mail: dhavalraval004@gmail.com

[2] Professor, Electrical Engineering Department, Vishwakarma Government Engineering College, Gujarat Technological University, Chadkheda, Ahmedabad, Gujarat, India

Received: Jun27, 2025 *Revised: Oct 24, 2025* *Accepted: Nov 14, 2025* *Available online: Jan 20, 2026*

***Abstract*—** The world is increasingly shifting towards cleaner renewable energy sources due to the environmental impact of conventional energy. Solar Photovoltaic (PV) technology holds immense promise as a future energy source, particularly through small-scale rooftop PV systems that can meet consumer demand and even generate surplus energy for additional income. However, integrating these systems into traditional distribution networks presents challenges in power quality. In networks with significant PV penetration, issues like local voltage rise and Reverse Power Flow (RPF) are becoming major concerns. India has varying maximum allowable PV capacity from state to state, ranging from 50% to 100%. This article focuses on analyzing the impact of PV system on voltage rise, using the IEEE 906 bus European LV distribution network as a case study. The study considers critical parameters such as the magnitude and duration of voltage rise, as well as specific locations where voltage rise issues arise. Solutions to mitigate voltage rise problems in PV-penetrated distribution networks are generalized to provide insights into the most preferable strategies for addressing voltage rise issues along with various power quality issues. Furthermore, to tackle the voltage rise problem, the integration of Volt/VAR control strategies is explored and evaluated for effectiveness using co-simulation techniques involving MATLAB and OpenDSS.

***Keywords*—** Rooftop PV generation; Power quality; Distribution network; Voltage rise; Volt/VAR.

1. INTRODUCTION

Advanced semiconductor technologies have revolutionized the photovoltaic (PV) industry by significantly reducing the cost of solar panel systems. These innovations empower residential consumers to harness clean energy while generating revenue through rooftop solar installations. In India, the state government of Gujarat has introduced a highly attractive subsidy scheme, offering financial assistance to encourage solar adoption. Specifically, the government provides a 40% subsidy for PV systems up to 3 kW and 20% for systems above 3 kW capacity, fostering both small- and large-scale residential installations.

While such initiatives promote sustainable energy, the integration of rooftop PV systems into existing distribution networks—originally designed for specific load profiles [1]—presents significant operational challenges. When PV systems are connected arbitrarily across consumer points, particularly under conditions of high generation and low demand, they disrupt traditional power flow patterns and introduce Reverse Power Flow (RPF). This, in turn, can lead to localized voltage rise and grid stability issues [2].

In addition to RPF, the intermittent nature of PV output causes frequent power fluctuations, contributing to voltage instability within distribution systems [3-7].

* Corresponding author
DOI: https://doi.org/10.5455/jjee.204-1750995874

For consumers sharing the same distribution transformer, the severity of voltage fluctuation is influenced by several factors—such as the size of the PV system, its distance from the transformer, and the length of shared conductors. Interestingly, voltage variations caused by a single PV unit, even in the absence of RPF, can sometimes exceed those from multiple PV systems with RPF [3]. Studies from high PV-penetrated countries show that the integration of large consumer-level PV systems can cause substantial voltage rises not only at the source terminal but also in adjacent network zones [4].

Compounding the issue is the uneven distribution of PV installations across three-phase systems, which aggravates pre-existing voltage imbalance due to unequal load demand. This imbalance can lead to increased power losses, malfunctioning relays (due to negative and zero-sequence currents), inaccurate measurements, and reduced transformer/motor lifespan [5].

It also introduces greater stress on rectifier components, distorts the supply's power factor [6], and contributes to the elevation of Neutral-to-Ground Voltage (NGV)—a phenomenon particularly critical when neutral conductors are overloaded [7]. When neutral impedance is non-negligible, excessive neutral currents can also generate common mode noise, breaching vendor-specified NGV safety thresholds, typically under 0.5–3 V RMS [8].

Traditional mitigation techniques—such as load balancing, conductor resizing, enhanced grounding, or the use of isolation transformers, though widely studied [9], have often proven inadequate under dynamic PV loading conditions.

Conventional voltage control devices such as On-Load Tap Changers (OLTC) [10-12], Line Voltage Regulators (LVR) [13, 14], and power-electronics-based compensators like STATCOM [15] and D-STATCOM [16-19], offer partial remedies. Coordinated control strategies, e.g., OLTC with D-STATCOM [19], attempt to maintain voltage within tight bands, with D-STATCOM providing reactive compensation beyond OLTC's tap-changing limits. Emerging studies further advocate the direct involvement of PV inverters in grid voltage regulation [20, 21].

However, such approaches often require significant investments in battery storage, controller infrastructure, and smart grid coordination. Static VAR compensators and current nullifiers also face practical challenges in terms of sizing, responsiveness, and scalability, especially in high-density PV deployment scenarios. In response, IEEE 1547 recommends that PV inverters connected to the grid incorporate Volt/VAR control functionality.

In support of this paradigm, numerous studies have investigated Volt/VAR-enabled inverters for improving power quality in distribution networks. A consolidated overview of these efforts is presented in Table 1, summarizing their objectives, test networks, and simulation environments.

This study advances the state of the art by evaluating Volt/VAR-enabled PV integration on a large, realistic IEEE 906-bus European LV network, rather than the small, stylized feeders commonly used in prior work. It employs a MATLAB–OpenDSS co-simulation with minute-level time resolution to jointly quantify both the magnitude and the duration of voltage rise—metrics that are rarely assessed together.

In what follows, Section 2 discusses generalized power quality issues in PV-integrated networks and critically analyzes existing mitigation strategies. Section 3 investigates voltage rise challenges specific to the IEEE 906-bus LV network. Section 4 validates the application of Volt/VAR-enabled PV inverters as a targeted solution.

Table 1. Review of key studies on distribution system optimization: Summary, test networks, and tools.

Reference	Study Summary	Test Network	Software Tools
[22]	Developed a reactive power controller to mitigate overvoltage due to high PV output. Performance compared using 720 time-series operating points.	IEEE 13-bus	MATLAB, OpenDSS
[23]	Proposed lateral-level Volt/VAR control using probabilistic models for minimizing active power losses and managing over-voltages.	IEEE 13-bus	MATLAB, OpenDSS
[24]	Introduced a two-stage stochastic optimization model for optimal smart inverter placement with Volt/VAR control to reduce voltage violations and minimize costs.	Arizona utility feeder	PySP (Pyomo), Gurobi 9.03
[25]	Focused on IEEE Std. 1547-2018 compliant Volt/VAR control using smart inverters to reduce energy losses and optimize distribution system efficiency.	IEEE 123-bus	MATLAB, OpenDSS
[26]	Developed a closed-loop reconfiguration strategy with Volt/VAR control and voltage-dependent models to enhance PV hosting and reduce CO_2 emissions.	IEEE 33-bus, IEEE 85-bus	AMPL, CPLEX 20.1.0
[27]	Combined conservation voltage reduction (CVR) and PV inverter controls to reduce substation demand while maintaining voltage within ANSI limits.	IEEE 8500-node	MATLAB, OpenDSS
[28]	Presented a scenario-generation method for day-ahead Volt/VAR control that improves solution efficiency by generating key voltage scenarios.	Custom radial feeder	MATLAB, CPLEX 12.7
[29]	Investigated how Volt/VAR control influences the lifespan of distribution transformers, with a model estimating transformer life loss.	IIT-Roorkee Distribution System	MATLAB, OpenDSS
[30]	Proposed Volt/VAR optimization with OLTC, VRs, and CBs to reduce substation apparent power and energy losses under DG and harmonics.	IEEE 33-bus	MATLAB, OpenDSS
[31]	Analyzed how different load models affect energy losses and VVC scheduling within a Volt/VAR optimization framework.	IEEE 123-node	MATLAB, OpenDSS

2. GENERALIZED OVERVIEW OF POWER QUALITY ISSUES IN PV-INTEGRATED DISTRIBUTION NETWORKS AND ANALYSIS OF EXISTING SOLUTIONS

In this section, a generalized representation of a PV-integrated distribution network is presented. The section provides an in-depth discussion of the issues that arise when integrating PV systems into distribution networks. It systematically categorizes various solutions available to mitigate these power quality challenges and elaborates on the capabilities of each solution. These approaches collectively provide a comprehensive understanding of how each mitigation technique contributes to improving the performance and reliability of PV-integrated distribution networks.

2.1. LV Distribution Network after PV Integration

Figures 1 and 2 depict a generalized overview of an LV distribution network influenced by PV generation. The secondary distribution network exhibits imbalances in both voltage and current owing to the presence of uneven load demand and PV generation. Here, I_A, I_B, I_C and i_a, i_b, i_c represent the primary distribution network currents and secondary distribution network currents, respectively. In a similar manner, V_A, V_B, V_C and v_a, v_b, v_c represent the

primary distribution voltages and secondary distribution voltages, respectively. Figure 3 shows the presence of positive-sequence (I^+), negative-sequence (I^-), and zero-sequence (I^0) components in the secondary distribution network. The secondary current can be expressed as:

$$I_{secondary} = I^{+}_{abc} + I^{-}_{abc} + I^{0}_{abc}$$

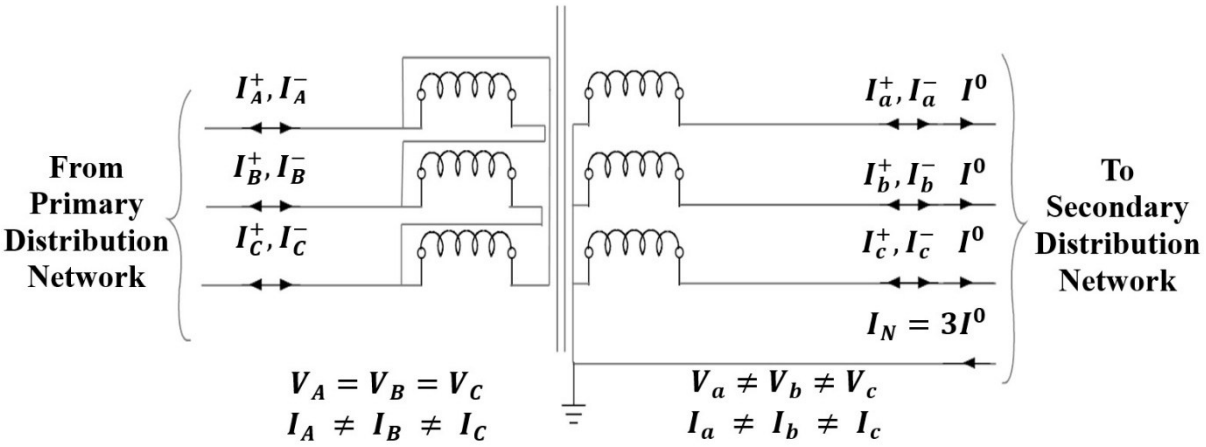

Fig. 1. PV Integrated distribution network.

With the PV system injecting power into the secondary distribution network, the net active demand $Re(I^+, I^-)$ of the network decreases. Consequently, this reduction impacts the power factor observed at the distribution transformer. The presence of neutral current I_N—inherent in an unbalanced current scenario across all three phases of the secondary distribution network—leads to the introduction of a neutral-to-ground voltage V_{NG}.

The high turns ratio of the step-down transformer helps mitigate voltage imbalance on the primary distribution side. Distribution transformers are generally configured as Δ–Y, which blocks zero-sequence currents and further suppresses imbalance propagation from the secondary to the primary. Thus, consistent with the schematic, the primary distribution network predominantly carries positive-sequence current $I^+$and negative-sequence current I^-. Notably, I^-can adversely affect protection equipment and lead to relay maloperation.

$$I_{primary} = I^{+}_{ABC} + I^{-}_{ABC} \tag{1}$$

2.2. Power Quality Improvement Using Power Electronics Without Energy Storage (S1)

Compensation devices without energy storage, as shown in Fig. 2, provide control over the imaginary current $Im(I)$, zero-sequence current I^0, and higher-frequency components of the real current $Re(\tilde{I})$. The neutral current I_N, which arises due to the presence of zero-sequence current I^0, can be eliminated by using a three-phase four-wire configuration of the compensating device. The compensation current can be expressed as:

$$I_{compensation} = Re(\tilde{I}_{abc}) + Im(I_{abc}) + I^0 \tag{2}$$

In the absence of energy storage, the compensator cannot control the unbalanced fundamental real current Re($\bar{I}$), which further propagates toward the primary side of the distribution transformer. Thus, the primary current becomes:

$$I_{primary} = Re(I^{+}_{ABC}) + Re(I^{-}_{ABC}) \tag{3}$$

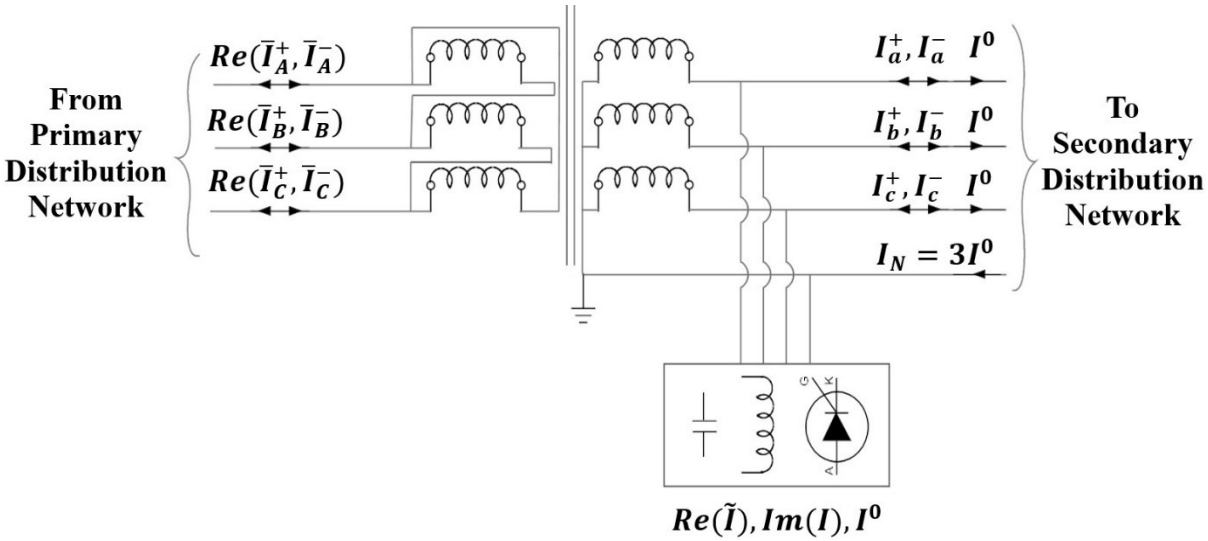

Fig. 2. Power quality improvement device without energy storage.

This topology enables the distribution network to operate at unity power factor by compensating the reactive power demand. Additionally, its capability to mitigate high-frequency current components leads to a reduction in total harmonic distortion (THD) within the distribution network. However, the suppression of reverse power flow remains challenging due to the absence of active power control. While voltage regulation at the point of common coupling (PCC) is achievable, maintaining appropriate voltage levels for individual consumers is not feasible under this configuration.

2.3. Power Quality Improvement Using Power Electronics with Energy Storage (S2)

The inclusion of energy storage allows the compensator to control unbalanced active current, which is generally not possible in compensators with only temporary energy storage (i.e., passive elements). In this context, the compensator can mitigate the high-frequency component of the real current $Re(\tilde{I}^+)$, the imaginary current $Im(I^+)$, the negative-sequence current I^-, and the zero-sequence current I^0. The compensation current can thus be expressed as:

$$I_{compensation} = Re(\tilde{I}_{abc}) + Im(I_{abc}) + I_{abc}^- + I^0 \quad (4)$$

With an adequately sized energy storage system, the primary side of the distribution transformer carries only the positive-sequence real current component $Re(\bar{I}^+)$, i.e.,

$$I_{primary} = Re(I_{ABC}^+) \quad (5)$$

This topology enables the management of both reactive and active power, effectively resolving a wide range of operational issues. It facilitates the correction of low power factor operation, mitigates voltage fluctuations such as rises and dips, and strategically balances active power to address challenges like reverse power flow.

This comprehensive functionality ensures network stability and minimizes the adverse effects of surplus or deficit active power. In addition to its primary capabilities, this topology inherently reduces total harmonic distortion (THD) by actively compensating for harmonic components within the system. While it is possible to regulate the voltage at the point of common coupling, the control over the voltage levels for individual consumers is not achievable.

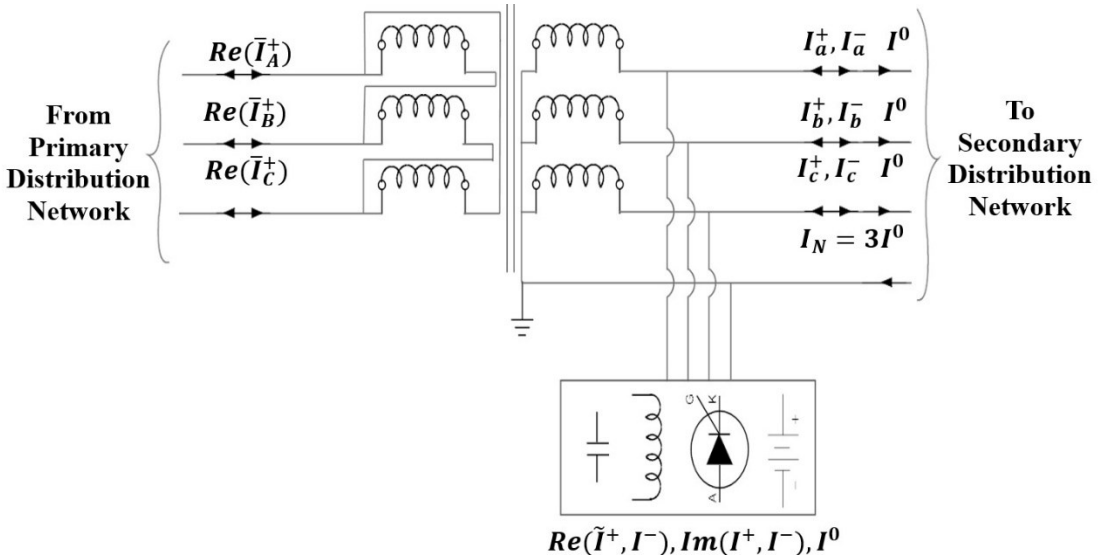

Fig. 3. Power quality improvement device with energy storage.

2.4. Power Quality Improvement via Phase Shifting of Load and PV Generation (S3)

In this topology, individual node voltage can be controlled, as power can be distributed among the phases by shifting load or generation. Voltage balance can be achieved to some extent within the secondary distribution network ($v_a \approx v_b \approx v_c$). However, achieving zero neutral current is contingent upon attaining perfect power balance, see Fig. 4.

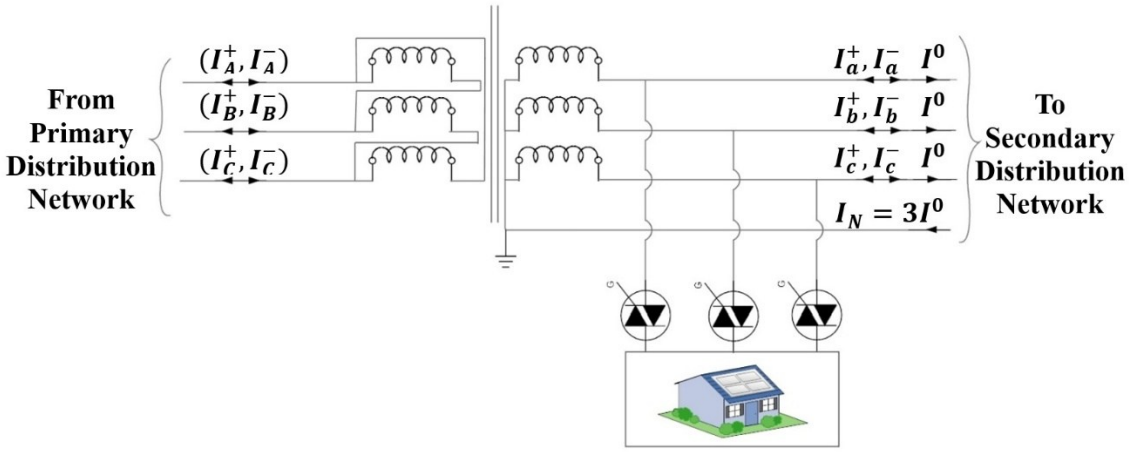

Fig. 4. Power quality improvement using phase shifting of load/PV generation.

$$I_N = 0 \; if \; S_x = \frac{S_{total}}{3} \; (x = a, b, c) \tag{6}$$

where S_x is the apparent power of phase x, and S_{total} is the total apparent power of the distribution network.

It is important to note that this solution requires the availability of three-phase conductors to facilitate power diversion among the phases. This requirement can increase the overall system cost. Furthermore, this topology does not provide control over harmonics or power factors.

2.5. Power Quality Improvements using PV Systems (S4)

In a distribution network with significant penetration of photovoltaic (PV) systems, the primary cause of power quality issues predominantly stems from imbalances in active power

distribution. Additionally, the widespread placement of PV systems throughout the network introduces voltage rise concerns.

To address these challenges, power quality improvement functionalities such as volt–var and volt–watt provide distributed solutions within the network. When these functionalities are directly integrated into PV systems, their effectiveness and reach are further extended across the distribution network.

Specifically, the volt–watt functionality presents two possible implementations. It either necessitates the addition of energy storage—which invariably increases system cost—or it relies on power curtailment strategies, as proposed in [24], which unfortunately result in active power losses. In contrast, the volt–var functionality optimally utilizes the available capacity of PV inverters to inject or absorb reactive power from the network, without requiring any additional costly components.

2.6. Comparative Analysis of Power Quality Improvement Topologies

In addressing the power quality challenges stemming from the rapid expansion of PV networks—particularly in regions such as India—it is evident that these challenges escalate with increased rooftop PV deployment. A critical consideration in formulating effective solutions is scalability. Topologies S-1 and S-2, being centralized three-phase solutions, face limitations in addressing distributed voltage rise and pose difficulties in large-scale deployment. Conversely, S-3 and S-4 represent single-phase distributed solutions which, although limited in sequence current control, offer enhanced scalability and flexibility. Their distributed implementation enables more effective management of voltage rise in highly PV-penetrated networks, positioning them as promising approaches for evolving distribution infrastructure, see Table 2.

Table 2. Summary of available solutions for mitigation of power quality issues in PV-penetrated distribution networks.

Top.	Re($\tilde{I}^{+}$)	Re($\tilde{I}^{-}$)	Im(I^{+})	Im(I^{-})	I_N	$\tilde{I}$	Voltage Rise	Harm.	P. Factor	RPF	Future Exp.
S-1	✗	✗	✓	✓	✗	✓	PCC	✗	✓	✗	Difficult
S-2	✓	✓	✓	✓	✗	✓	PCC	✓	✓	✓	Difficult
S-3	✓	✗	✗	✗	✗	✗	Dist.	✗	✗	✓	Easy
S-4	✓	✓	✓	✓	✓	✓	Dist.	✓	✓	✓	Easy

3. INTEGRATION OF PV WITH THE IEEE 906-BUS EUROPEAN LV NETWORK AND POWER QUALITY ISSUES

The modified IEEE 906-bus European Low Voltage (LV) distribution network is depicted in Fig. 5. This network comprises 55 single-phase consumers distributed across different phases. The default load profiles are adopted as provided in the IEEE test case. For this study, Phase A is considered to evaluate the impact of rooftop PV integration, and all subsequent analysis is focused exclusively on its consumers.

The load demand characteristics of these consumers are summarized in Table 3. The maximum, minimum, and average load demands (in kW) across a 24-hour period are tabulated. Notably, Consumer 29 exhibits high variability, with demand ranging from 0.054 kW to 10.549 kW in a single day.

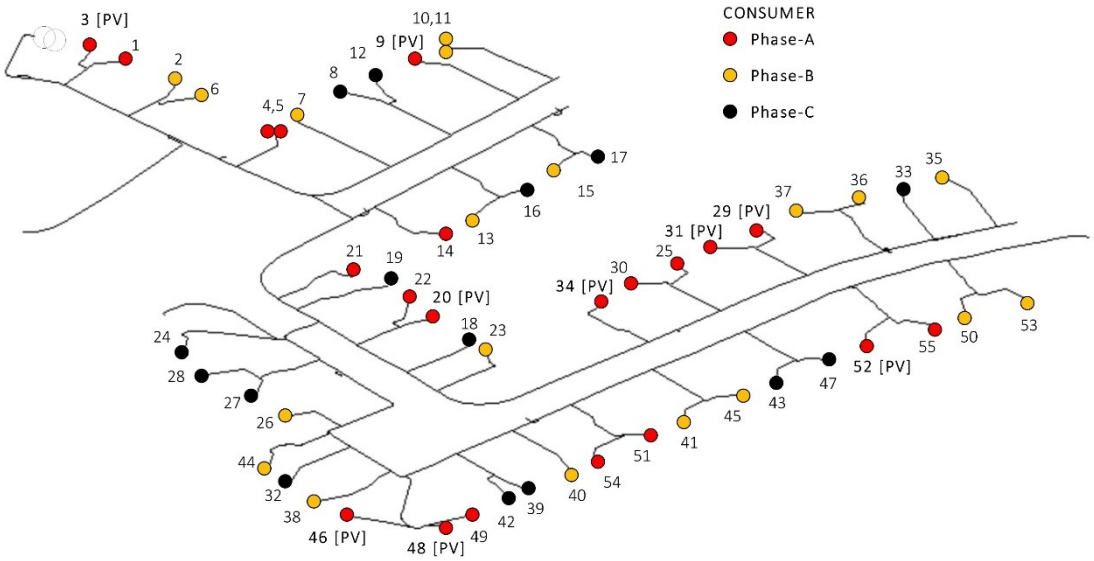

Fig. 5. Modified IEEE 906-Bus European LV distribution network.

Table 3. Power demand analysis of individual consumers in phase-A.

Consumer Number	Max [kW]	Min [kW]	Average [kW]
1	2.771	0.036	0.426
3*	8.308	0.054	0.2842
4	5.18	0.048	0.409
5	3.438	0.035	0.2895
9*	6.84	0.059	0.28063
14	2.471	0.049	0.2246
20*	6.223	0.048	0.5417
21	3.067	0.045	0.24
22	1.383	0.045	0.204
25	3.32	0.053	0.279
29*	10.549	0.054	0.5234
30	3.044	0.053	0.2837
31*	8.297	0.053	0.2888
34*	8.566	0.045	0.2508
46*	7.844	0.049	0.4001
48*	8.894	0.046	0.446
49	3.485	0.044	0.3344
51	3.566	0.053	0.3459
52*	8.267	0.052	0.2437
54	3.299	0.048	0.3919
55	2.901	0.055	0.3003

* Indicates consumers selected for PV integration due to higher maximum demand.

3.1. Selection of Consumers for PV Integration

The selection of a rooftop photovoltaic (PV) system is commonly favored for consumers with substantial power demands. During the analysis of consumer demand, particular attention is given to customers exhibiting high maximum power requirements as they present a considerable opportunity for adopting rooftop PV installations. As highlighted in Table 3,

nine consumers with larger power demand have been considered for integration of rooftop PV systems based on the consumer's maximum demand.

3.2. Sizing of PV Systems

PV system capacity allocation in India varies according to state-specific regulations. Table 4 outlines the percentage of sanctioned load permissible for rooftop PV installations across different regions. Accordingly, three cases are formulated for this study: Case 1 (50% of sanctioned load), Case 2 (80% of sanctioned load), and Case 3 (100% of sanctioned load).

Table 4. Allowed capacity of rooftop PV systems in Indian States*.

Sanctioned Load [%]	Applicable States
50	Gujarat, Madhya Pradesh, Jammu and Kashmir
80	Punjab, Rajasthan, Uttarakhand, Uttar Pradesh, Andhra Pradesh, Himachal Pradesh
100	Maharashtra, Manipur, Mizoram, Nagaland, Odisha, Sikkim, Tamil Nadu, Telangana, Tripura, Delhi, Assam, Bihar, Chhattisgarh, Goa and all UTs, Haryana, Jharkhand, Karnataka, Kerala, Meghalaya, Chandigarh

*Source: MYSUN – Statewise Rooftop Solar Policies in India. https://www.itsmysun.com/solar-state-wise-policy/.

3.3. Impact of PV Integration on Voltage Profile

Table 5 presents the voltage profile of consumers in Phase A under different PV penetration scenarios (50%, 80%, and 100% of the sanctioned load) in comparison with the base case (before PV integration). The data indicate that PV penetration initially improves the minimum voltage levels due to reduced feeder loading; however, it simultaneously introduces voltage rise concerns, particularly at higher penetration levels.

At 50% PV penetration, all consumers maintain voltage magnitudes within the permissible limit of ±6% (0.94–1.06 p.u.). This suggests that moderate PV integration supports voltage improvement without violating operational standards. However, at 80% penetration, several consumers start to approach or slightly exceed the upper voltage limit (1.06 p.u.), reflecting the onset of localized overvoltage conditions caused by reverse power flow from distributed PV units.

The 100% PV penetration scenario (Case 3) exhibits the most significant deviation, with 18 out of 21 consumers exceeding the upper acceptable voltage threshold. Consumers such as C20, C25, C29, C31, and C52 experience the highest voltages ranging from 1.11 p.u. to 1.13 p.u., confirming that excessive PV generation without adequate voltage regulation leads to pronounced overvoltage issues.

Figure 6 illustrates the temporal variation of voltages for individual consumers between 10:00 and 17:00 hours. Consumers with similar secondary line lengths exhibit correlated voltage behavior, such as (C4, C5), (C29, C31), and (C51, C54). This correlation highlights the spatial dependency of voltage variations, emphasizing that the electrical location of consumers significantly influences voltage performance. Hence, voltage control strategies must account for both the spatial distribution of PV units and load density to ensure network-wide voltage stability.

Table 5. Analysis of voltage profile of consumers in phase A.

Consumer	(Before PV Integration)		50% of Sanctioned Load		80% of Sanctioned Load		100% of Sanctioned Load	
	Lowest	Highest	Lowest	Highest	Lowest	Highest	Lowest	Highest
1	0.9886	1.0033	0.9905	1.013	0.9905	1.022	0.9905	1.0281
3*	0.9875	1.0034	0.9905	1.0135	0.9905	1.0228	0.9905	1.0291
4	0.9832	1.0097	0.982	1.0264	0.982	1.0452	0.982	1.0578
5	0.9835	1.0097	0.9823	1.0262	0.9823	1.0449	0.9823	1.0575
9*	0.9785	1.0125	0.9773	1.0329	0.9773	1.0558	0.9773	1.0717
14	0.9792	1.0139	0.9779	1.0334	0.9779	1.0575	0.9779	1.0737
20*	0.9732	1.0179	0.9719	1.0432	0.9719	1.0746	0.9719	1.0955
21	0.9751	1.0166	0.9738	1.0391	0.9738	1.0675	0.9738	1.0864
22	0.9735	1.0179	0.9722	1.0429	0.9722	1.0742	0.9722	1.0949
25	0.9653	1.0218	0.9671	1.0527	0.9684	1.0913	0.9684	1.1172
29*	0.9584	1.0227	0.9599	1.0567	0.9693	1.0983	0.9693	1.1262
30	0.9653	1.0218	0.9671	1.0527	0.9687	1.0913	0.9687	1.1172
31*	0.96	1.0227	0.9611	1.0566	0.9693	1.0981	0.9693	1.1259
34*	0.9677	1.0211	0.9695	1.0525	0.9698	1.0908	0.9698	1.1165
46*	0.9636	1.0192	0.9666	1.0483	0.9666	1.084	0.9666	1.1072
48*	0.9653	1.019	0.9658	1.0482	0.9658	1.0836	0.9658	1.1067
49	0.9653	1.0191	0.9663	1.048	0.9663	1.0833	0.9663	1.1063
51	0.9654	1.0203	0.9688	1.0483	0.9688	1.0815	0.9688	1.1041
52*	0.964	1.0215	0.9681	1.0528	0.9681	1.0884	0.9681	1.1129
54	0.9656	1.0203	0.969	1.0482	0.969	1.0814	0.969	1.1041
55	0.9653	1.0215	0.9678	1.0524	0.9678	1.0875	0.9678	1.1117

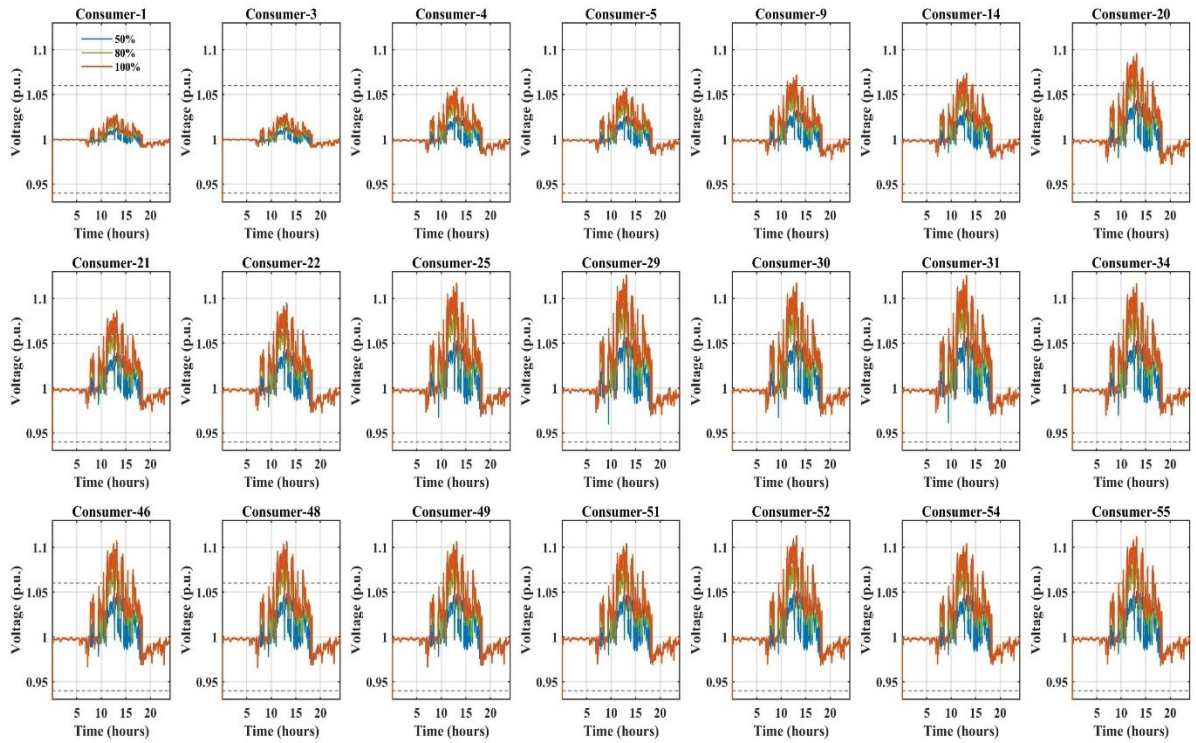

Fig. 6. Voltage profile of individual consumers in phase-A (10:00--17:00).

Table 6 summarizes the duration of voltage limit exceedance for all consumers at 80% and 100% PV penetration levels. At 80% penetration, a few consumers (notably C20, C25, C29, C31, and C52) experience short exceedance durations ranging from 53 to 159 minutes, indicating intermittent overvoltage occurrences. In contrast, at 100% PV penetration, the exceedance durations increase substantially, with most consumers showing prolonged overvoltage periods exceeding 150 minutes.

Among them, Consumer 29 exhibits the highest exceedance duration of 208 minutes, followed closely by C31 (207 minutes) and C20 (148 minutes). These prolonged durations can be attributed to the consumers' electrical proximity to the substation and relatively large PV generation capacities, which induce reverse power flow during midday peak generation hours.

From these observations, it is evident that higher PV penetration levels intensify both the magnitude and duration of voltage rise across the distribution network. Therefore, Case 3 (100% PV penetration) is identified as the worst-case operating condition and is selected for further detailed analysis and the development of voltage regulation strategies. Addressing this extreme case ensures that the proposed mitigation measures remain effective under the most critical and heavily stressed operating scenarios.

Table 6. Duration of Voltage Limit Exceedance (in minutes).

Consumer	**1**	**3**	**4**	**5**	**9**	**14**	**20**	**21**	**22**	**25**	**29**	**30**	**31**	**34**	**46**	**48**	**49**	**51**	**52**	**54**	**55**
Time (80%)	0	0	0	0	0	0	53	19	49	123	159	124	158	123	94	92	92	89	119	89	115
Time (100%)	0	0	0	0	34	55	148	107	145	191	208	191	207	191	181	180	179	176	192	176	191

It is also important to note that external factors such as ambient temperature variations, cloud movement, and shading conditions inherently influence PV generation and, consequently, voltage behavior across the network. Although these factors were not explicitly analyzed in the present study, their effect was indirectly represented through the use of variable irradiance profiles during simulation. Since irradiance variability captures the dynamic fluctuations in PV output caused by temperature and weather changes, the simulated conditions effectively replicate the real-world voltage behavior observed under such environmental influences.

4. VOLT/VAR CONTROL INTEGRATION WITH PV SYSTEM FOR VOLTAGE RISE MITIGATION

Figure 7 illustrates the Volt/VAR control characteristic adopted for the rooftop photovoltaic (PV) system in accordance with the IEEE 1547 standard. The Volt/VAR curve defines the functional relationship between the inverter's reactive power output and the terminal voltage, enabling autonomous voltage regulation within the distribution feeder.

The Volt/VAR curve incorporates a dead band between V_{LD} and V_{HD} , typically corresponding to ±1% of the nominal voltage, which effectively prevents frequent and unnecessary switching of the inverter's reactive power response.

Within this region, the reactive power remains zero, allowing stable operation around the nominal voltage. When the terminal voltage falls below V_{LD}or rises above V_{HD}, the inverter begins a linear variation of reactive power: capacitive injection between V_{LD} and V_L , and inductive absorption between $V_{HD}$and V_H, see Table 7.

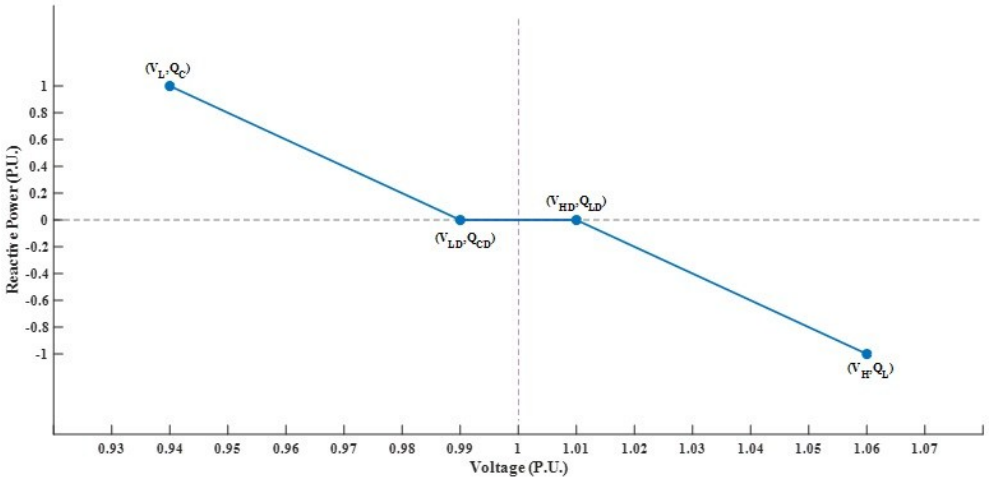

Fig. 7. Volt/VAR curve of the rooftop photovoltaic system based on IEEE~1547 standard.

Table 7. Volt/VAR parameters and corresponding settings.

Parameter	Definition	Selected Setting
$(\boldsymbol{V_L})$	Lower voltage limit	$(V_{rated} - 0.06\,V_{rated})$
$(\boldsymbol{Q_C})$	Capacitive reactive power at lower voltage limit	100% of available inverter capacity
$(\boldsymbol{V_{LD}})$	Dead-band lower voltage limit	$(V_{rated} - 0.01\,V_{rated})$
$(\boldsymbol{Q_{CD}})$	Reactive power injection at (V_{LD})	0
$(\boldsymbol{V_{HD}})$	Dead-band upper voltage limit	$(V_{rated} + 0.01\,V_{rated})$
$(\boldsymbol{Q_{LD}})$	Reactive power absorption at (V_{HD})	0
$(\boldsymbol{V_H})$	Upper voltage limit	$(V_{rated} + 0.06\,V_{rated})$
$(\boldsymbol{Q_L})$	Inductive reactive power at upper voltage limit	100% of available inverter capacity

This linear droop characteristic ensures smooth and progressive changes in reactive power, preventing abrupt current transients that could otherwise disturb system stability. At the extreme voltage limits $V_L$and V_H(i.e., ±6% of V_{rated}), the inverter operates at its full reactive capacity, utilizing 100% of the available reactive power margin. Here, "available inverter capacity" refers to the portion of apparent power capability not occupied by active power delivery at any given instant. By leveraging the inverter's residual capacity for reactive regulation at voltage extremes, the system maintains voltage within statutory limits, thereby mitigating overvoltage and undervoltage conditions while enhancing overall feeder voltage stability.

5. RESULTS AND DISCUSSION

Figure 8 illustrates the reactive power injection and absorption patterns of individual photovoltaic (PV) systems governed by their Volt/VAR control characteristics. Each inverter autonomously adjusts its reactive power output based on the local voltage magnitude, thereby contributing to localized voltage regulation along the feeder. PV units located near the distribution transformer, such as PV Systems 2, 3, and 5, experience minimal voltage deviations and therefore exhibit comparatively lower reactive power activity. Their output remains close to unity power factor for most of the day, indicating that voltage rise is insignificant in their vicinity owing to low feeder impedance. In contrast, far-end PV units corresponding to Consumers 29 and 31 demonstrate pronounced reactive power absorption during peak irradiance hours. These systems experience elevated voltages exceeding the 1.01

p.u. deadband threshold, which triggers inductive reactive power absorption as per the Volt/VAR droop control characteristic.

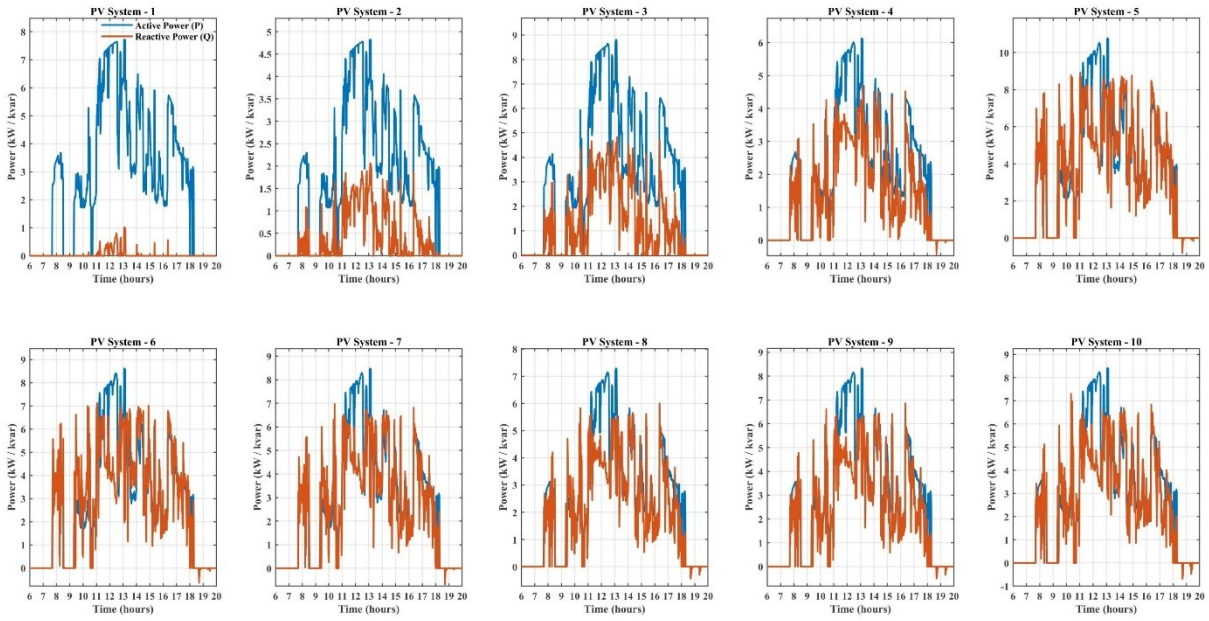

Fig. 8. Volt/VAR control integration with PV system for voltage rise mitigation.

Table 8 presents a comparative voltage profile analysis of Phase-A consumers before and after the implementation of Volt/VAR control. The data clearly indicates that the application of inverter-based reactive control results in a substantial reduction in both voltage rise magnitude and the duration of over-voltage occurrences. The maximum voltage magnitude observed across the feeder decreased by approximately 1.0–1.25%, while the minimum voltage levels remained practically unchanged. The average improvement in voltage uniformity for far-end consumers beyond node 25 is around 5%, whereas near-end consumers exhibit marginal changes due to their inherently stable voltage profiles.

Among all consumers, Consumer 29 displayed the most significant enhancement with a 5.67% reduction in maximum voltage magnitude and a 93% reduction in violation duration (from 191 minutes to 14 minutes). This improvement can be attributed to the combined reactive power absorption provided by its own PV inverter and that of the adjacent Consumer 31, both situated in the high-voltage section of the feeder. Similarly, PV-equipped nodes such as Consumers 9, 14, 20, and 21 exhibited complete mitigation of voltage violations, achieving a 100% reduction in exceedance duration. For instance, at Consumer 14, the duration of voltage rise decreased from 55 minutes to zero, corresponding to total elimination of over-voltage. These findings demonstrate that Volt/VAR control effectively suppresses transient voltage excursions during periods of fluctuating solar generation.

Mid-feeder PV-integrated consumers such as 46, 48, 49, 51, and 52 also showed substantial improvements, with voltage reduction percentages of approximately 4.6–5.1% and violation duration reductions exceeding 95%. Specifically, the duration at Consumer 52 declined from 179 minutes to just 2 minutes (98.95% reduction). Non-PV consumers such as 25 and 55 also benefited, though to a lesser degree, with violation durations decreasing from 145 to 2 minutes (98.95%) and from 192 to 1 minute (99.48%), respectively. Overall, Volt/VAR integration led to an average violation duration reduction exceeding 90% across the network,

confirming the strong temporal efficacy of inverter-based reactive power management, see Table 8.

Table 8. Voltage profile analysis of phase-A consumers after Volt/VAR integration.

Consumer	Min (After PV)	Max (After PV)	Duration [min]	Min (Volt/VAR)	Max (Volt/VAR)	Duration [min]	% Improvement	% Duration Reduction
2*	0.9918	1.0236	0	0.9907	1.0113	0	1.23	100
3*	0.9918	1.0246	0	0.9908	1.0121	0	1.25	100
4	0.9832	1.0516	0	0.9824	1.0276	0	2.4	100
5	0.9835	1.0516	0	0.9837	1.0276	0	2.4	100
9*	0.9782	1.0699	34	0.9774	1.0385	0	3.14	100
14	0.9792	1.0699	55	0.9745	1.0385	0	3.14	100
20*	0.9732	1.0941	148	0.9714	1.0519	0	3.84	100
21	0.9751	1.0841	107	0.9745	1.0463	0	3.78	100
25*	0.9696	1.1177	145	0.9668	1.0651	2	5.26	98.95
29*	0.9703	1.1177	191	0.9671	1.0709	14	5.67	92.95
30	0.97	1.1177	208	0.9671	1.0652	4	5.26	98.43
31*	0.9706	1.1272	191	0.9671	1.0707	14	5.66	92.89
46*	0.9677	1.1079	207	0.9674	1.0595	4	4.84	98.43
48*	0.9668	1.1072	191	0.9674	1.0648	0	4.84	100
49	0.9673	1.1067	181	0.9671	1.0588	0	4.67	100
51	0.9671	1.1074	180	0.9671	1.0573	0	4.6	100
52*	0.9649	1.1136	179	0.9671	1.0628	2	5.07	98.95
54	0.9703	1.104	176	0.9687	1.0573	0	4.67	100
55	0.969	1.1123	192	0.9664	1.0621	1	5.02	99.48

*Indicates PV-integrated consumers

Notes:

% **Improvement** is computed from the reduction in the **Max** value (p.u.).

% **Duration Reduction** and new durations are calculated relative to pre-control exceedance.

Figure 9 shows the variation of RMS voltage with time, highlighting the temporal benefits of Volt/VAR control. The results confirm that the control mechanism not only mitigates voltage rise during midday high-generation periods but also alleviates under-voltage conditions during late-afternoon load peaks between 15:00 and 17:00 hours. This dual capability is achieved through bidirectional inverter operation: injecting capacitive reactive power when voltage falls below the 0.99 p.u. threshold and absorbing inductive reactive power when it exceeds 1.01 p.u. Consequently, system voltages remain within the statutory range throughout the day, ensuring both over-voltage suppression and under-voltage compensation. Figure 10(a) provides a comparative visualization of voltage deviation before and after Volt/VAR implementation, clearly validating the improvement in voltage stability across the Phase-A section of the distribution network. Following Volt/VAR activation, the overall voltage deviation remains within ±0.05 p.u., demonstrating a stable and balanced voltage profile along the feeder.

Figure 10(b) presents the reduction in the duration of voltage limit violations for all monitored consumers, confirming the temporal effectiveness of the Volt/VAR scheme. Most consumers exhibit more than a 90% decrease in violation duration, while PV-integrated nodes achieve near-complete mitigation. The magnitude of temporal reduction correlates directly with the level of reactive power participation observed in Figure 7.

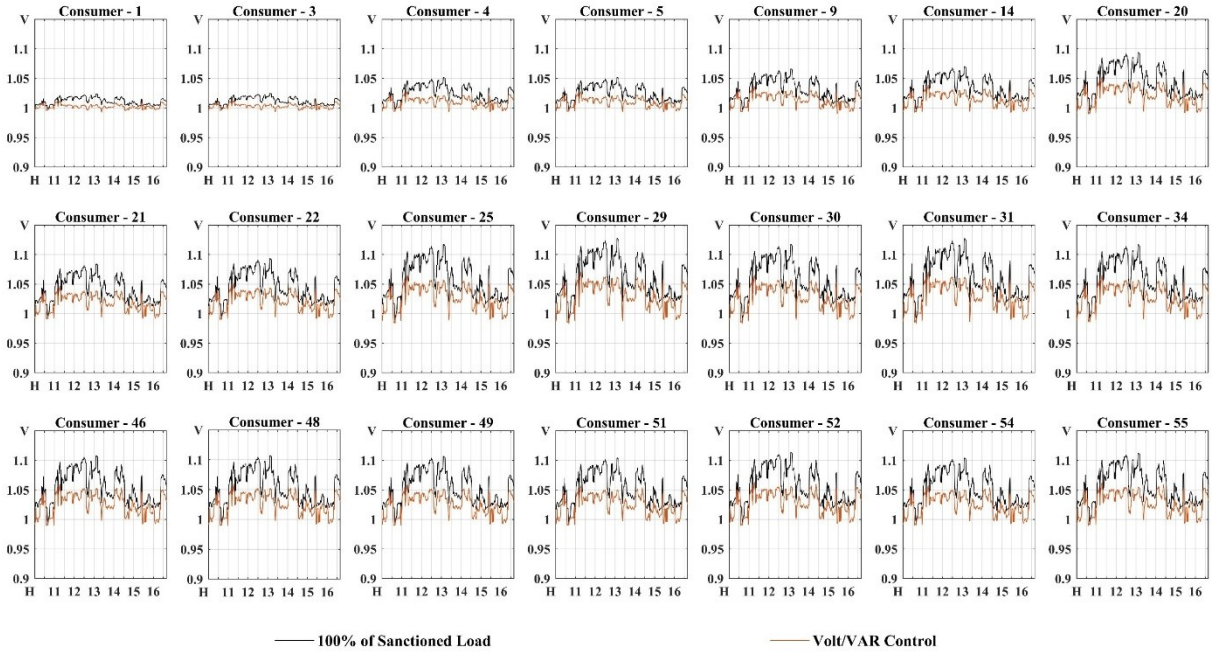

Fig. 9. Voltage profile of individual consumers in phase-A after Volt/VAR control.

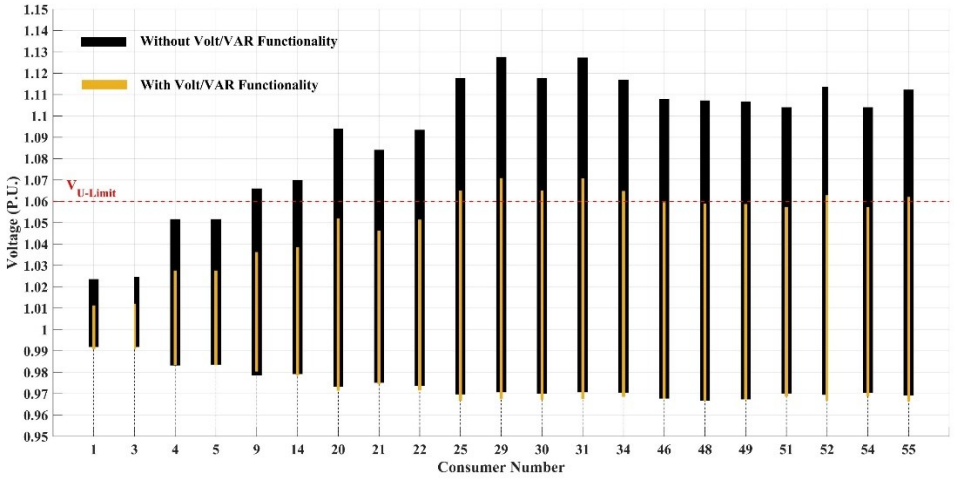

(a) Voltage deviation in distribution network.

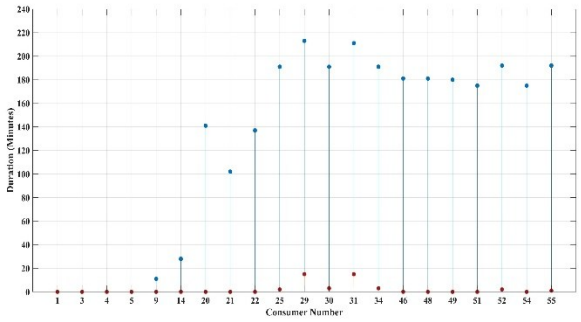

(b) Time duration of voltage rise.

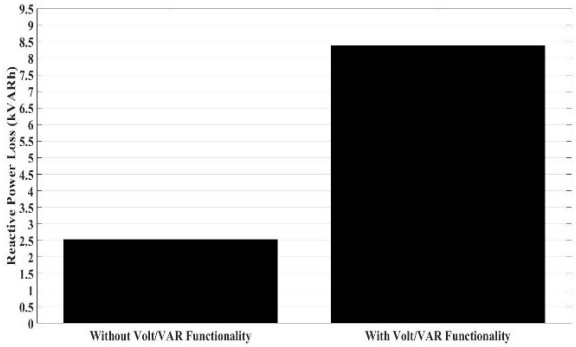

(c) Reactive power loss in distribution network.

Fig. 10. Comparison of reactive power loss and voltage rise duration for each consumer before and after Volt/VAR control implementation.

Figure 10(c) quantifies the network-level impact of Volt/VAR functionality by comparing the cumulative reactive power losses recorded throughout the simulation period. The total reactive power loss without Volt/VAR functionality was measured at 2.5233 kVARh,

whereas the introduction of Volt/VAR control increased this value to 8.3790 kVARh. This indicates that although the Volt/VAR strategy substantially improves voltage stability and minimizes voltage rise violations, it does so at the expense of higher reactive power circulation within the network. Nevertheless, this trade-off is generally considered acceptable in distribution systems, as the overall voltage quality, system reliability, and hosting capacity for distributed PV units are significantly improved despite the marginal increase in reactive losses.

6. CONCLUSIONS

This study establishes that inverter-based Volt/VAR functionality provides a technically robust and operationally feasible solution for mitigating voltage rise in low-voltage distribution networks with high photovoltaic (PV) penetration. By enabling autonomous, localized reactive power exchange, Volt/VAR control effectively suppresses over-voltage conditions and enhances voltage uniformity across the feeder. The analysis revealed marked reductions in both the magnitude and duration of voltage deviations, with several PV-integrated consumers achieving complete elimination of voltage violations and far-end nodes demonstrating average voltage improvements of approximately five percent. These outcomes confirm that decentralized reactive power control substantially strengthens voltage stability and extends the PV hosting capacity of existing networks.

However, the improved voltage performance is accompanied by an increase in reactive energy losses, which rose from approximately 2.5 kVARh to 8.4 kVARh following Volt/VAR implementation. This increase reflects the continual reactive compensation required to maintain bus voltages within statutory limits, underscoring the inherent trade-off between voltage regulation and network efficiency. Despite this, the overall enhancement in power quality and reliability justifies the additional reactive power circulation from a system-wide perspective.

From a practical standpoint, the integration of Volt/VAR-enabled inverters is both technologically and economically viable, as most commercial PV inverters already comply with international standards such as IEEE 1547-2018 and IEC 62116. Implementation costs are marginal and primarily involve firmware configuration and system coordination. The approach is inherently scalable and well-suited for gradual adoption in developing power systems such as those in India. Nevertheless, successful large-scale deployment will require supportive regulatory mechanisms, interoperability standards, and incentive frameworks that recognize the ancillary voltage support provided by distributed energy resources.

In summary, Volt/VAR functionality represents an efficient, regulation-aligned, and cost-effective strategy for enhancing voltage stability in PV-rich distribution networks. Future research should aim to develop coordinated, adaptive, or optimization-driven Volt/VAR schemes that balance reactive power utilization with network efficiency, enabling the reliable and sustainable integration of renewable generation into modern smart grids.

REFERENCES

1. T. Gönen, C. Ten, A. Mehrizi-Sani, *Electric Power Distribution Engineering,* CRC Press, 2024.
2. D. Raval, S. Pandya, “Phase shifting strategy for mitigation of local voltage rise in highly PV penetrated distribution network,” 9th IEEE International Conference on Power Systems, 2021, doi: 10.1109/ICPS52420.2021.9670088.

3. A. Parchure, S. Tyler, A. Peskin, K. Rahimi, R. Broadwater, M. Dilek, "Investigating PV generation induced voltage volatility for customers sharing a distribution service transformer," *IEEE Transactions on Industry Applications*, vol. 53, no. 1, pp. 71–79, 2016, doi: 10.1109/TIA.2016.2610949.
4. M. Bajaj, A. Singh, "Grid integrated renewable DG systems: A review of power quality challenges and state-of-the-art mitigation techniques," *International Journal of Energy Research*, vol. 44, no. 1, pp. 26–69, 2020, doi: 10.1002/er.4847.
5. T. Chen, C. Yang, T. Hsieh, "Case studies of the impact of voltage imbalance on power distribution systems and equipment," Proceedings of the WSEAS International Conference on Mathematics and Computers in Science and Engineering, 2009.
6. B. Bennett, "Unbalanced voltage supply: The damaging effects on three-phase induction motors and rectifiers," *ABB Power Conditioning – Electrification Products Division*, 2017, https://search.abb.com/library/Download.aspx?DocumentID=2UCD401218-P&LanguageCode=en&DocumentPartId=&Action=Launch.
7. J. Balda, A. Oliva, D. McNabb, R. Richardson, "Measurements of neutral currents and voltages on a distribution feeder," *IEEE Transactions on Power Delivery*, vol. 12, no. 4, pp. 1799–1804, 1997, doi: 10.1109/61.634208.
8. T. Gruzs, "A survey of neutral currents in three-phase computer power systems," Industrial and Commercial Power Systems Technical Conference, 1989, doi: 10.1109/ICPS.1989.37245.
9. M. Alam, K. Muttaqi, D. Sutanto, "Community energy storage for neutral voltage rise mitigation in four-wire multigrounded LV feeders with unbalanced solar PV allocation," *IEEE Transactions on Smart Grid*, vol. 6, no. 6, pp. 2845–2855, 2015, doi: 10.1109/TSG.2015.2427872
10. C. Gao, M. Redfern, "A review of voltage control techniques of networks with distributed generations using on-load tap changer transformers," 45th International Universities Power Engineering Conference, 2010.
11. C. Sarimuthu, V. Ramachandaramurthy, K. Agileswari, H. Mokhlis, "A review on voltage control methods using on-load tap changer transformers for networks with renewable energy sources," *Renewable and Sustainable Energy Reviews*, vol. 62, pp. 1154–1161, 2016, doi: 10.1016/j.rser.2016.05.016.
12. J. Iria, M. Heleno, G. Cardoso, "Optimal sizing and placement of energy storage systems and on-load tap changer transformers in distribution networks," *Applied Energy*, vol. 250, pp. 1147–1157, 2019, doi: 10.1016/j.apenergy.2019.04.120.
13. R. Jahn, M. Holt, C. Rehtanz, "Mitigation of voltage unbalances using a line voltage regulator," IEEE Madrid PowerTech, 2021, doi: 10.1109/PowerTech46648.2021.9494930.
14. M. Holt, C. Rehtanz, "Optimizing line-voltage regulators with regard to power quality," *Electric Power Systems Research*, vol. 190, p. 106654, 2021, doi: 10.1016/j.epsr.2020.106654.
15. K. Chenchireddy, V. Kumar, K. Sreejyothi, P. Tejaswi, "A review on D-STATCOM control techniques for power quality improvement in distribution," 5th International Conference on Electronics, Communication and Aerospace Technology, 2021, doi: 10.1109/ICECA52323.2021.9676019.
16. C. Chen, "Enhancement of PV penetration with DSTATCOM in Taipower distribution system," *IEEE Transactions on Power Systems*, vol. 28, no. 2, pp. 1560–1567, 2013, doi: 10.1109/TPWRS.2012.2226063.
17. B. Zad, "Improvement of OLTC performance in voltage regulation of MV distribution systems with DG using D-STATCOM," 22nd International Conference and Exhibition on Electricity Distribution, 2013, doi: 10.1049/cp.2013.0762.
18. S. M. Fazeli, "Individual-phase control of 3-phase 4-wire voltage–source converter," *IET Power Electronics*, vol. 7, no. 9, pp. 2354–2364, 2014, doi: 10.1049/iet-pel.2013.0973.

19. N. Efkarpidis, "Coordinated voltage control scheme for Flemish LV grids utilizing OLTC transformers and D-STATCOMs,'' 12th IET International Conference on Developments in Power System Protection, 2014, doi: 10.1049/cp.2014.0041.
20. S. Pukhrem, "Enhanced network voltage management techniques under proliferation of rooftop PV," *IEEE Journal of Emerging and Selected Topics in Power Electronics*, vol. 5, no. 2, pp. 889–898, 2017, doi: 10.1109/JESTPE.2016.2614986.
21. D. Raval, P. Munjani, N. Mansoori, "Reference based maximum power point tracking algorithm for photovoltaic power generation,'' International Conference on Electrical Power and Energy Systems, 2016. doi: 10.1109/ICEPES.2016.7915971.
22. F. Aboshady, "Sequentially coordinated and cooperative volt/var control of PV inverters in distribution networks," *Electronics*, vol. 12, no. 8, p. 1765, 2023, doi: 10.3390/electronics12081765.
23. F. Aboshady, "Reactive power control of PV inverters in active distribution grids with high PV penetration," *IEEE Access*, vol. 11, pp. 81477–81496, 2023, doi: 10.1109/ACCESS.2023.3299351.
24. M. Chen, "Optimal placement of PV smart inverters with volt–var control," *IEEE Systems Journal*, vol. 17, no. 3, pp. 3436–3446, 2023, doi: 10.1109/JSYST.2023.3256121.
25. S. Satsangi, G. Kumbhar, "Energy savings estimation of a distribution system with intelligent Volt–VAR control," *CSEE Journal of Power and Energy Systems*, vol. 8, no. 5, pp. 1477–1486, 2022, doi: 10.17775/CSEEJPES.2021.08340.
26. J. Home-Ortiz, "Increasing RES hosting capacity using reconfiguration and Volt/VAR control," *IEEE Transactions on Industry Applications*, vol. 58, no. 4, pp. 4424–4435, 2022, doi: 10.1109/TIA.2022.3177175.
27. S. Arora, "Substation demand reduction by CVR-enabled intelligent PV inverter functions," *International Transactions on Electrical Energy Systems*, vol. 31, no. 2, 2021, doi: 10.1002/2050-7038.12724.
28. Z. Xiong, "A day-ahead chance-constrained Volt/VAR control scheme," *IEEE Access*, vol. 9, pp. 64033–64042, 2021, doi: 10.1109/ACCESS.2021.3074649.
29. K. Kumar, S. Satsangi, G. Kumbhar, "Extension of life of distribution transformer using Volt–VAR optimisation," *IET Generation, Transmission & Distribution*, vol. 13, no. 10, pp. 1777–1785, 2019, doi: 10.1049/iet-gtd.2018.5746.
30. S. Satsangi, G. Kumbhar, "Integrated Volt–VAR optimization with distributed energy sources," *Electric Power Components and Systems*, vol. 46, pp. 1522–1539, 2018, doi: 10.1080/15325008.2018.1511004
31. S. Satsangi, G. Kumbhar, "Effect of load models on scheduling of VVC devices," *IET Generation, Transmission & Distribution*, vol. 12, no. 17, pp. 3993–4001, 2018, doi: 10.1049/iet-gtd.2018.5262.